

PAPER

Direct-Sequence/Spread-Spectrum Communication System with Sampling Rate Selection Diversity

Yohei SUZUKI^{†a)}, Anas M. BOSTAMAM^{†b)}, Mamiko INAMORI^{†c)}, *Student Members*,
and Yukitoshi SANADA^{†d)}, *Member*

SUMMARY In this paper, sampling rate selection diversity (SRSD) scheme for Direct-Sequence/Spread-Spectrum (DS/SS) is proposed. In DS/SS communication systems, oversampling may be employed to increase the signal-to-noise ratio (SNR). However, oversampling enlarges the power consumption because signal processing of the receiver has to be carried out at a higher clock rate. Higher sampling rate does not always maximize the SNR. In the proposed SRSD scheme, the power consumption can be reduced by selecting the optimum sampling rate depending on the characteristics of the channel. The proposed SRSD scheme can also reduce the BER more than the conventional oversampling scheme under certain channel conditions.

key words: oversampling, diversity, direct-sequence/spread-spectrum (DS/SS), RAKE receiver, multipath channel, cognitive radio

1. Introduction

DS/SS has recently become a mainstream technology for wireless communication systems, such as Wideband-Code Division Multiple Access (W-CDMA), or IEEE802.11b Wireless Local Area Network (WLAN). In the DS/SS system, a RAKE receiver is used to improve the BER performance. The RAKE receiver can gather more signal energy and achieve multipath diversity.

In [1] the effect of tap spacing on the RAKE receiver has been evaluated, particularly when the received signal is sampled at higher than the Nyquist rate. The BER can be then reduced when the sampling rate is high. However, the tap positions and the sampling rate are fixed regardless of the characteristics of the channel in the conventional scheme. The RAKE receiver with oversampling can not always gather the largest signal energy. Furthermore, the power consumption of the RAKE receiver becomes high in proportion to the sampling rate.

In order to reduce the power consumption, the sampling rate should be low. In this paper, the SRSD scheme is proposed to reduce the average oversampling rate without degradation of the BER. The proposed scheme selects the tap positions and the sampling rate depending on the characteristics of the channel. When the delay spread is large, signal energy can be gathered even if the sampling rate is

low. This is because the RAKE receiver is able to cover the dominant multipath. On the other hand, when the delay spread is small, the RAKE receiver with higher oversampling rate works effectively. Therefore, the sampling rate is selected to maximize the SNR [3], [4].

In this paper, the proposed SRSD scheme in IEEE802.11b is simulated. The BER of the proposed scheme is compared with the conventional scheme in which the tap positions and the oversampling rate, are fixed and the probability of the sampling rate reduction is evaluated. The total power consumption may be reduced in proportion to this probability.

This paper is organized as follows. Section 2 gives the system and channel models. In Sect. 3, the proposed schemes are explained. Section 4 shows the numerical results through computer simulation. Section 5 gives our conclusions.

2. System and Channel Model

2.1 System Model

Figure 1 shows a system model used in this paper. The IEEE802.11b baseband model for the case of one user is assumed [3], [4]. The transmitted signal is expressed as

$$x(t) = \sqrt{E_b} \sum_{i=-\infty}^{+\infty} \frac{s(i)}{\sqrt{N}} \sum_{n=0}^{N-1} c(n)p(t - nT_c - iT) \quad (1)$$

where E_b is the average symbol energy, T is the symbol period, $s(i)$ is the i th BPSK symbol (± 1), T_c is the chip period, $\{c(n); n = 1, \dots, 11\}$ is the 11 chip Barker code, $p(t)$ is the chip pulse shape, and N is the spreading factor ($= 11$) [6], [7]. The chip pulse is filtered by a root raised cosine filter with the rolloff factor of 0.5.

The received signal can be expressed as

$$r(t) = \sum_{l=1}^L g_l \otimes x(t - \tau) + n(t) \quad (2)$$

where \otimes denotes the convolutional operation, g_l is the channel impulse response of the l th path, L is the number of paths, and $n(t)$ is the additive white Gaussian noise (AWGN).

The tap spacing of the RAKE receiver is not integer times of the chip duration when the received signal is oversampled. The noise components of the signal on all the taps

Manuscript received December 11, 2006.

Manuscript revised June 14, 2007.

[†]The authors are with the Dept. of Electronics and Electrical Engineering, Keio University, Yokohama-shi, 223-8522 Japan.

a) E-mail: suzuki@snd.elec.keio.ac.jp

b) E-mail: anas@snd.elec.keio.ac.jp

c) E-mail: mamiko@snd.elec.keio.ac.jp

d) E-mail: sanada@elec.keio.ac.jp

DOI: 10.1093/ietcom/e91-b.1.267

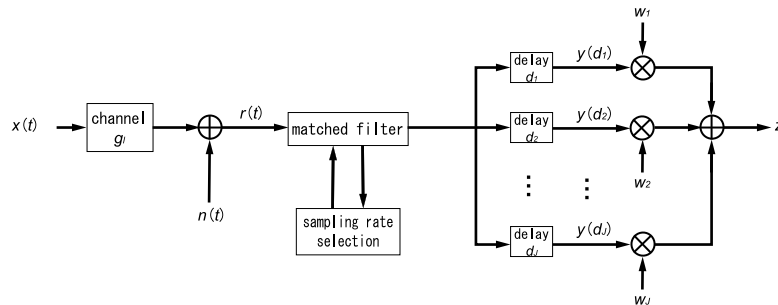


Fig. 1 System model.

are correlated to each other. To solve this problem, the optimum combining rule of the RAKE receiver has been proposed in [3].

The received signal is despread by the matched filter. The spreading waveform $a(t)$ can be expressed as

$$a(t) = \frac{1}{\sqrt{N}} \sum_{n=0}^{N-1} c(n)p(t - nT_c). \quad (3)$$

From Eqs. (2) and (3), the output of the matched filter can be written as

$$y(d_j) = \sum_{m=0}^{MN-1} r_s(m + d_j)a_s(m) \quad (4)$$

where $r_s(m) = r(m\frac{T_c}{M})$, $a_s(m) = a(m\frac{T_c}{M})$, and $\{d_j; j = 1, \dots, J\}$ is the delay of the j th tap of the RAKE receiver, M is the oversampling ratio. J is the number of taps. d_j is varied depending on the oversampling rate. The despread signals are combined using the optimum combining weights $\text{red}\mathbf{w} = [w_1, w_2, \dots, w_J]^T$. The output value of RAKE receiver can be expressed as

$$z = \mathbf{w}^H \mathbf{y} \quad (5)$$

where $\mathbf{y} = [y(d_1), y(d_2), \dots, y(d_J)]^T$, \mathbf{H} denotes the Hermitian transform. \mathbf{y} can be expressed as

$$\mathbf{y} = \mathbf{h}\mathbf{s}(i) + \mathbf{u} \quad (6)$$

where \mathbf{h} is the vector of values corresponding to the symbol of interest, the elements of the vector \mathbf{h} are the apparent complex gain of each branch, and \mathbf{u} models the overall noise (noise and interference). \mathbf{h} can be approximated as

$$\mathbf{h} \approx \mathbf{B}\mathbf{g} \quad (7)$$

where $\mathbf{g} = [g_1, g_2, \dots, g_J]^T$ and \mathbf{B} is $J \times L$ matrix whose element in the i th row and j th column is $r_p(d_i - d_j)$ [3]. $r_p(m)$ is the deterministic autocorrelation function for the sampled chip pulse shape $p_s(m)$. $J \times J$ matrix \mathbf{R} which is the covariance matrix of \mathbf{u} is similar to \mathbf{B} . The elements of \mathbf{R} can be approximated by $r_p(d_i - d_j)$.

Based on an maximum likelihood (ML) approach \mathbf{w} can be expressed as

$$\mathbf{w} = \mathbf{R}^{-1} \mathbf{h}. \quad (8)$$

In this combining rule of the RAKE receiver, the filtered noise can be whitened.

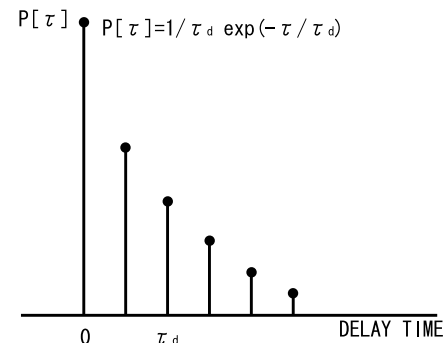


Fig. 2 Path delay profile for an exponential channel model.

Table 1 Indoor residential JTC channel model.

	Channel A	Channel B
τ_d [ns]	18	70
A [dB]	18.9	20.3

2.2 Channel Model

In this paper, an uniform channel model and an exponential channel model are employed. The exponential channel model is recommended in IEEE802.11. This model represents a real world scenario in which the positions of the reflectors generate paths that have longer delay [8]. As shown in Fig. 2, the path delay profile for this model has the form: $P[\tau] = 1/\tau_d \exp(-\tau/\tau_d)$ where the parameter τ_d completely characterizes the path delay profile. For the exponential model, the maximum excess delay:

$$\tau_m = \frac{A \times \tau_d}{10 \times \log_{10}(e)},$$

where A is the amplitude of the smallest noticeable amplitude given in dB relative to the amplitude of the 0th delay (line of sight) path.

In this paper, τ_d and A are set based on the JTC model which is presented in 1994 by the Joint Standards Committee (JTC) [9], [10]. Tables 1 and 2 shows τ_d and A for the 2 different channels that compose the indoor residential and the indoor office JTC model respectively.

Table 2 Indoor office JTC channel model.

	Channel A	Channel B
τ_d [ns]	35	100
A [dB]	7.2	21.7

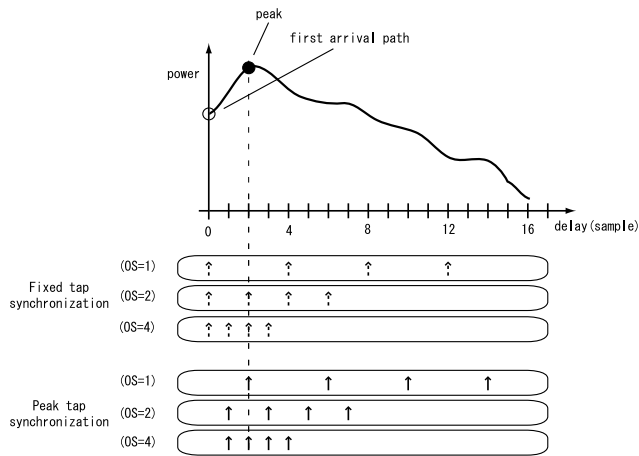


Fig. 3 Tap position.

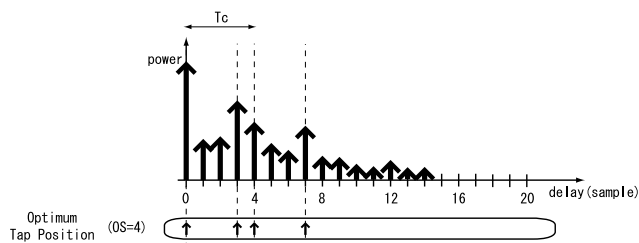


Fig. 4 Optimum tap placement.

2.3 Synchronization

The relation between the output of the matched filter and the tap positions is shown in Fig. 3. The output of the matched filter is averaged in terms of the corresponding phase of the spreading code during the preamble period. In the conventional scheme, “Fixed tap synchronization” is used. The first tap of the RAKE receiver is placed at the delay of the first arrival path.

The other scheme, called “Peak tap synchronization” is used in the proposed scheme. The synchronization with the received signal is achieved by detecting the peak of the matched filter output [5]. As shown in Fig. 3, the first tap of the RAKE receiver is placed at the maximum peak of the averaged matched filter output, when the oversampling rate is 1. The first tap is assumed to be placed at half or 1 sample before the maximum peak, when the oversampling rate is 2 and 4.

The optimum tap placement is also evaluated. The tap positions are selected according to the impulse response of the channel as shown in Fig. 4. In this paper, the SRSD scheme is proposed to reduce the power consumption. The

BER with the optimum tap placement may be better than the proposed SRSD scheme. However, the intervals between the taps are not always multiple of T_c with the optimum tap placement. Therefore, the oversampling rate may not be changed from 4 to 1, and the power consumption can not be reduced.

3. Sampling Rate Selection Diversity

3.1 Conventional Scheme

In [1] the effect of tap spacing on the RAKE receiver has been evaluated, particularly when the tap spacing is not integer times of the chip duration. By enlarging the number of taps in the RAKE receiver with a narrower tap spacing over the full range of the delay spread, the RAKE receiver can gather more signal energy and achieve multipath diversity. For this reason, the BER can be reduced when the sampling rate is high.

However, as the sampling rate becomes high and the number of taps increases, the complexity and the power consumption of the receiver also grow.

In the conventional scheme, the range of the delay spread that can be gathered by the RAKE receiver is fixed because oversampling rate is fixed. Therefore, the RAKE receiver may collect only the noise components of the signal or lose energy of the delay path according to the characteristics of the channel.

3.2 Proposed Scheme

The SRSD scheme is proposed to reduce the power consumption. The oversampling rate is selected in the preamble period of the packet and it is updated at the beginning of the data period. During the preamble period, the oversampling rate is set to the maximum. Only in the data period, the power consumption can be reduced by selecting the oversampling rate. When the data period is much longer than the preamble period, the power consumption can be sufficiently reduced in this proposed SRSD scheme.

The oversampling rate is selected to maximize the SNR depending on the characteristics of the channel. The SNR of the fading channel is given by [3]:

$$\text{SNR}(\mathbf{h}) = E_b/N_0 \mathbf{h}^H \mathbf{R}^{-1} \mathbf{h}. \tag{9}$$

$\text{SNR}(\mathbf{h})$ is estimated at each oversampling rate in the preamble period of the packet. The oversampling rate for the data signals is selected to maximize the SNR.

With the SRSD scheme, the BER can be reduced without increasing the number of taps of the RAKE receiver. It can also reduce the average oversampling rate which is relative to the power consumption.

4. Numerical Results

4.1 Simulation Conditions

The simulation conditions are shown in Table 3. BPSK is

employed as the modulation scheme. Barker code with the length of 11 is used for spreading. One packet consists of the preamble part of 128 bits and data part of 1000 bits. 10000 packets are simulated with different channel conditions. The channel state of each frame is assumed to be constant. The number of RAKE taps is set to 4.

In this paper, the power consumption of the matched filter is evaluated as it generally occupies the large amount of the total power consumption. Suppose that the matched filter is composed of CMOS circuits, the power consumption, P , is modeled by the following equation:

$$P = p_s \cdot f_c \cdot C_l \cdot V_{dd}^2 \quad (10)$$

where p_s is the switching probability, f_c is the clock frequency, C_l is the load capacitance and V_{dd} is the supply voltage [11]. f_c and C_l increase proportionally to the sampling rate. This means P is in proportion to the square of the sampling rate. Thus, it is assumed the power consumption of the CMOS circuits with the oversampling rate of 4 is 16 times higher than that with the oversampling rate of 1. The numerical results are normalized by the power consumption with the oversampling rate of 1.

Table 3 Simulation conditions.

Number of Trials	10000 times
Modulation Scheme	BPSK
Data Length	1000 bits
Preamble Length	128 bits
Transmitted Filter	root raised cosine filter
Received Filter	root raised cosine filter
Number of Taps	4
Number of Users	1
Spreading Sequence	Barker code
Sequence Length	11

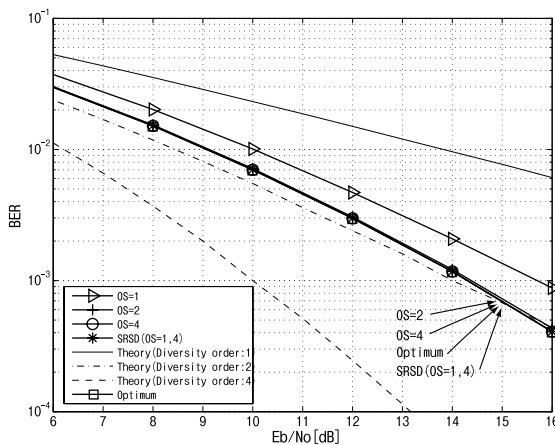


Fig. 5 BER vs. E_b/N_0 ; delay spread is T_c ; path interval is $0.25T_c$; Fixed tap synchronization.

4.2 Simulation Results

4.2.1 Effect of the Tap Position

In order to evaluate the relation between the tap position selection algorithms and the characteristics of the channel, independent multipath Rayleigh fading is assumed here. The number of multipath is set to 4 and uniform delay profile is employed.

Figures 5, 6, 7 and 8 depict the BER versus E_b/N_0 of the conventional scheme which employs the oversampling at the rate of 1, 2, and 4, the proposed scheme, and the optimum tap placement. “Theory” means the theoretical BER of BPSK modulation on a Rayleigh fading channel with diversity order 1, 2 and 4. The tap delay d_j is set to $\{1, 2, 3, 4\}$ for any oversampling rate. The delay spread and the path interval are set as T_c and $0.25T_c$ for Figs. 5 and 6, $4T_c$ and T_c for Figs. 7 and 8. Fixed tap synchronization is used in Figs. 5 and 7 and Peak tap synchronization is used in Figs. 6 and 8.

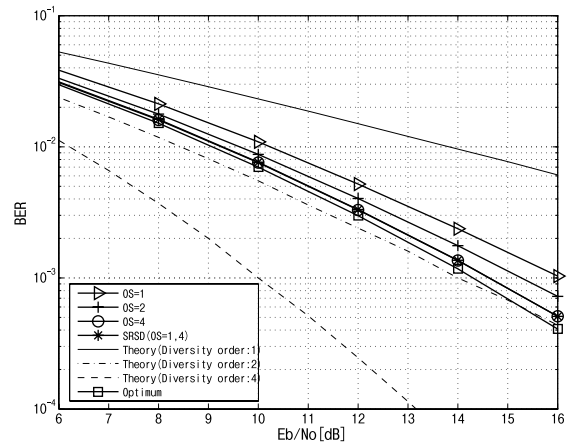


Fig. 6 BER vs. E_b/N_0 ; delay spread is T_c ; path interval is $0.25T_c$; Peak tap synchronization.

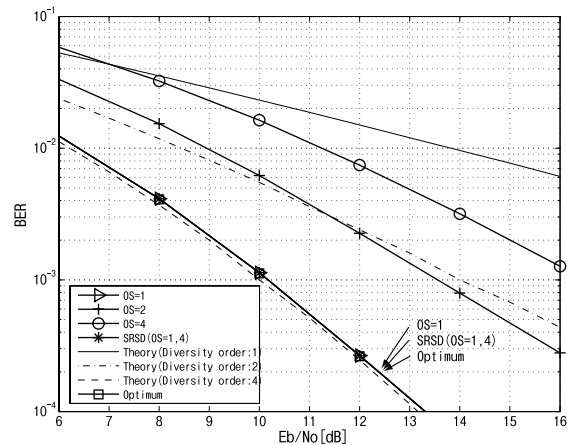


Fig. 7 BER vs. E_b/N_0 ; delay spread is $4T_c$; path interval is T_c ; Fixed tap synchronization.

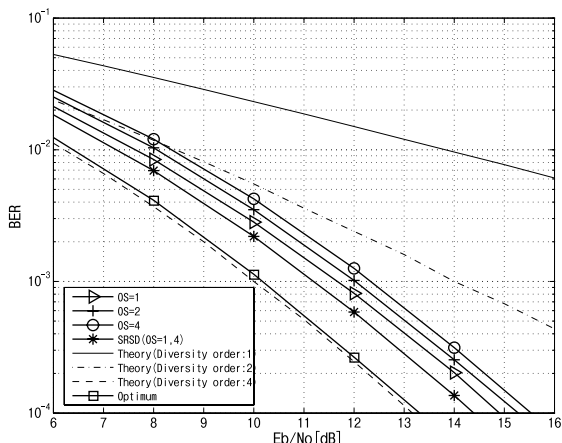


Fig. 8 BER vs. E_b/N_0 ; delay spread is $4T_c$; path interval is T_c ; Peak tap synchronization.

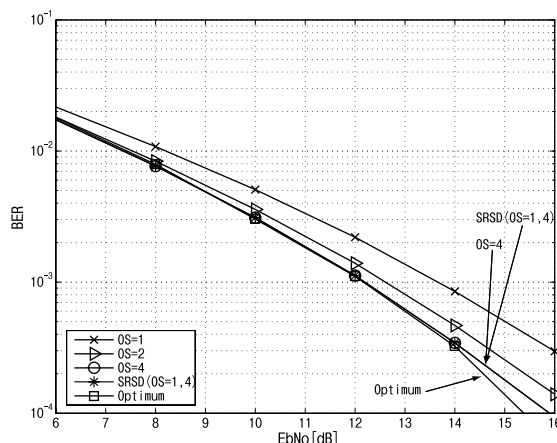


Fig. 9 BER vs. E_b/N_0 ; JTC indoor residential channel A.

Table 4 Probability of the sampling rate selection and the average power consumption: Channel model is rayleigh.

Delay Spread	Path Interval	Tap Placement	Sampling Rate Per Chip		Average Power Consumption
			1	4	
T_c	$0.25T_c$	Fixed	5.24%	94.76%	15.21
		Peak	22.91%	77.09%	12.56
$4T_c$	T_c	Fixed	100%	0%	1
		Peak	61.21%	38.79%	6.81

Table 4 shows the probability of the sampling rate selection and the average power consumption. When the oversampling rate of the data part is always 4, The normalized average power consumption is 16.

Comparing Fig. 5 with Fig. 6, and Fig. 7 with Fig. 8, the effect of the tap position is shown. From these results when the path interval is $0.25T_c$, the power consumption with Peak tap synchronization is better than that with Fixed tap synchronization while the BERs are almost the same. In this case with Peak tap synchronization the strongest path can be captured while it may be missed with Fixed tap synchronization as shown in Fig. 13(a).

However, when the path interval is T_c , the BER and the power consumption with Peak tap synchronization are worse than those with Fixed tap synchronization. This is because with Peak tap synchronization some of the taps may only collect the noise components if the tap spacing is T_c and the delay spread is $4T_c$ as shown in Fig. 13(b).

The rest of the results employs Peak tap synchronization as the practical channel models described in Sect. 2.2 have the delay spread of less than $2T_c$.

The BER with the optimum tap placement is better than the proposed SRSD scheme. However, the intervals between the taps are not always multiple of T_c with the optimum tap placement. Therefore, the oversampling rate may not be changed from 4 to 1, and the power consumption can not be reduced. Thus, the tap spacing is fixed in the proposed scheme.

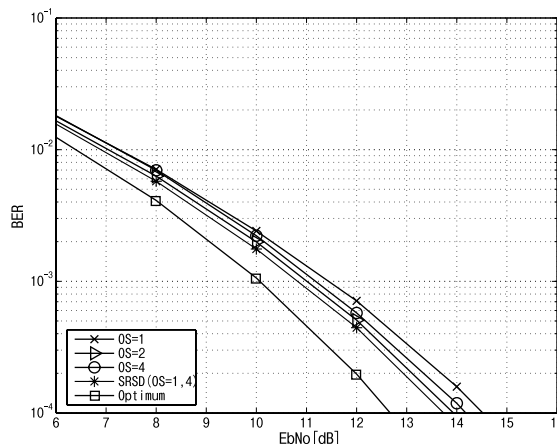


Fig. 10 BER vs. E_b/N_0 ; JTC indoor residential channel B.

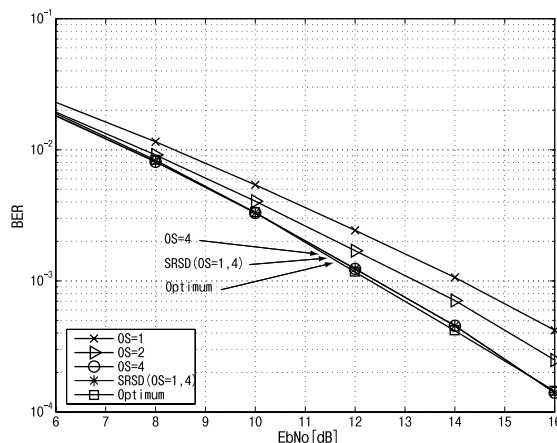


Fig. 11 BER vs. E_b/N_0 ; JTC indoor office channel A.

4.2.2 Relation between the Probability of the Sampling Rate Selection and the Characteristics of the Channel

The paths with small delay spread and large delay spread

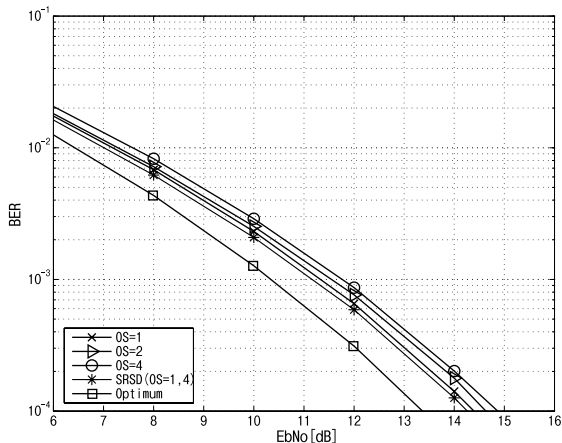


Fig. 12 BER vs. E_b/N_0 : JTC indoor office channel B.

Table 5 Probability of the sampling rate selection and the average power consumption: Channel model is the exponential channel model based on JTC indoor channel model.

Indoor Scenario	Channel Model	Sampling Rate Per Chip		Average Power Consumption
		1	4	
Indoor	Channel A	23.08%	76.92%	12.54
Residential	Channel B	59.07%	40.93%	7.14
Indoor	Channel A	24.66%	75.34%	12.30
Office	Channel B	68.74%	31.26%	5.69

are investigated in order to show the relation between the probability of sampling rate selection and the characteristics of the channel.

Figures 5 and 6 show that oversampling reduces the BER if the delay spread is small. The BER of the proposed SRSD scheme is similar to that of the conventional system with the oversampling rate of 4. The RAKE receiver can gather signal energy and achieve multipath diversity because the tap position is close to the path delays. In contrast, Figs. 7 and 8 show that oversampling deteriorates the BER. The RAKE receiver with the oversampling rate of 4 can not gather the signal energy or achieve multipath diversity because the tap delay is smaller than the path delay. However, the BER of the proposed SRSD scheme shows similar BER performance to that of the conventional system with the oversampling rate of 1 when the delay spread is large.

From these results, when the number of taps is fixed, the optimum sampling rate is depending on the characteristics of the channel and it should be selected in order to gather more signal energy and achieve multipath diversity.

4.2.3 BER of the Proposed SRSD Scheme under the Exponential Channel Model

In order to simulate the proposed SRSD scheme under the practical indoor channel model, the exponential channel model based on JTC indoor model are used [9], [10]. Figures 9, 10, 11 and 12 show the BER versus E_b/N_0 of the con-

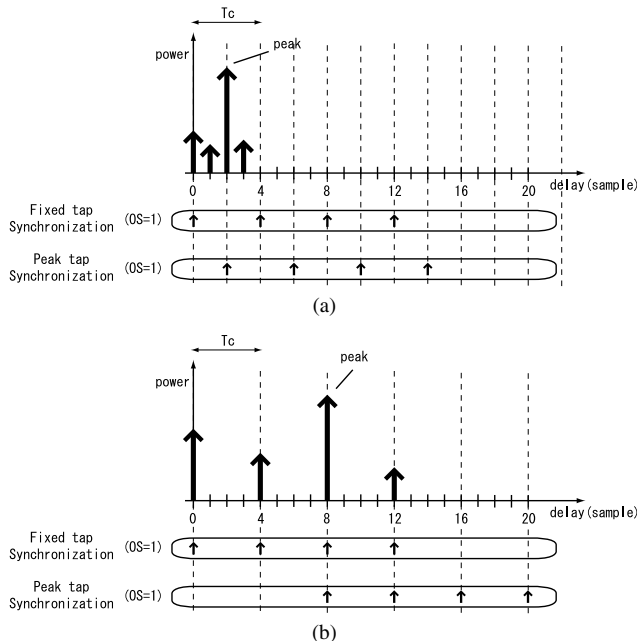


Fig. 13 Difference of tap placement algorithms; tap spacing is $0.25T_c$; delay spread is (a) T_c and (b) $4T_c$.

ventional system which employs oversampling at the rate of 1, 2, and 4, the proposed scheme, and the optimum tap placement. The tap delay d_j is set to $\{1, 2, 3, 4\}$ for any oversampling rate. The channel model of Figs. 9, 10, 11 and 12 are Indoor Residential Channel A, Indoor Residential Channel B, Indoor Office Channel A and Indoor Office Channel B. Table 5 shows the probability of the sampling rate selection and the average power consumption.

From these results, it is shown that, the BERs in Figs. 9 and 11 are similar to BER in Fig. 6. This means that the oversampling reduces the BER. This is because the delay spread of Indoor Residential Channel A and Indoor Office Channel A is small. From Table 5, the probability of selecting the sampling rate of 1 is 23.08[%] and 24.66[%] for Indoor Residential Channel A and Indoor Office Channel A, respectively. From Figs. 9 and 11, the proposed scheme improve the BER performance then reduce the average power consumption.

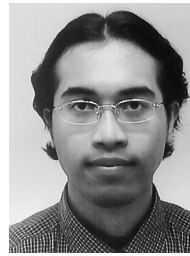
The BERs in Figs. 10 and 12 have the same tendency as BER in Fig. 8. It is shown that the oversampling deteriorates the BER. This is because the delay spread of Indoor Residential Channel B and Indoor Office Channel B is relatively large. As for the SRSD scheme, the probability of selecting the sampling rate of 1 is 59.07[%] and 68.74[%] for Indoor Residential Channel B and Indoor Office Channel B respectively. Accordingly, the averaged power consumption of the matched filter is 7.14 and 5.69 for Indoor Residential Channel B and Indoor Office Channel B, respectively. Therefore the proposed SRSD scheme under Indoor Residential Channel B and Indoor Office Channel B can reduce the power consumption.

5. Conclusions

In this paper, the DS/SS with SRSD scheme has been proposed. It has been shown that, the proposed SRSD scheme can achieve the best BER under any channel conditions. It has also been shown that this SRSD scheme is able to reduce the power consumption in terms of the same BER.

References

- [1] K.J. Kim, S.Y. Kwon, E.K. Hong, and K.C. Whang, "Effect of tap spacing on the performance of direct-sequence spread-spectrum RAKE receiver," *IEEE Trans. Commun.*, vol.48, no.6, pp.1029–1036, June 2000.
- [2] B. Soltanian, V. Lehinén, E.S. Lohan, and M. Renfors, "Complexity analysis of an interpolation based rake receiver for WCDMA systems," *IEEE GLOBECOM 2001*, vol.6, pp.3528–3532, Nov. 2001.
- [3] C. Cozzo, G.E. Bottomley, and A.S. Khayrallah, "Rake receiver finger placement for realistic channels," *IEEE WCNC. 2004*, vol.1, pp.316–321, March 2004.
- [4] G.E. Bottomley, T. Ottosson, and Y.E. Wang, "A generalized RAKE receiver for interference suppression," *IEEE J. Sel. Areas Commun.*, vol.18, no.8, pp.1536–1545, Aug. 2000.
- [5] T. Chunjiang, Z. xin, L. Bo-an, and C. Hongyi, "The design of 802.11b WLAN baseband processor," *Proc. 5th International Conference on ASIC.*, vol.2, pp.852–855, Oct. 2003.
- [6] IEEE Standard 802.11b-1999.
- [7] IEEE Std 802.11b-1999 Cor 1-2001.
- [8] N. Chayat, "Tentative criteria for comparison of modulation methods," *IEEE P802.11-97/96*, Sept. 1997.
- [9] Joint Technical Committee of Committee T1 R1p1.4 and TIA R46.3.3/TR 45.4.4 on Wireless Access, Draft Final Report on RF Channel Characterization, Paper no.JTC (AIR)/94.01.17-238r4, Jan. 17, 1994.
- [10] M.G. Laffin, "Draft final technical report on RF channel characterization and system deployment modeling," Joint Technical Committee, JTC(AIR)/94.08.01-065R4, 1994.
- [11] S. Goto, T. Yamada, N. Takayama, Y. Matsushita, Y. Harada, and H. Yasuura, "A design for a low-power digital matched filter applicable to W-CDMA," *Digital System Design, Proceedings. Euromicro Symposium*, pp.210–217 Sept. 2002.



Anas Muhamad Bostamam was born in Pahang, Malaysia in 1981. He received his B.E. and M.E. degrees in electronics engineering from Keio University, Japan in 2004 and 2005 respectively. Since September 2005, he has been a Ph.D. candidate in School of Integrated Design Engineering, Graduate School of Science and Technology, Keio University. His research interests are mainly concentrated on software defined radio.



Mamiko Inamori was born in Kagoshima, Japan in 1982. She received her B.E. degree in electronics engineering from Keio University, Japan in 2005. Since April 2005, she has been a graduate student in School of Integrated Design Engineering, Graduate School of Science and Technology, Keio University. Her research interests are mainly concentrated on software defined radio.



Yukitoshi Sanada was born in Tokyo in 1969. He received his B.E. degree in electrical engineering from Keio University, Yokohama Japan, his M.A.Sc. degree in electrical engineering from the University of Victoria, B.C., Canada, and his Ph.D. degree in electrical engineering from Keio University, Yokohama Japan, in 1992, 1995, and 1997, respectively. In 1997 he joined the Faculty of Engineering, Tokyo Institute of Technology as a Research Associate. In 2000 he joined Advanced Telecommunication Laboratory, Sony Computer Science Laboratories, Inc, as an associate researcher. In 2001 he joined Faculty of Science and Engineering, Keio University, where he is now an assistant professor. He received the Young Engineer Award from IEICE Japan in 1997. His current research interest is in software defined radio and ultra wideband systems.



Yohei Suzuki was born in Tokyo, Japan in 1983. He received his B.E. degree in electronics engineering from Keio University, Japan in 2006. Since April 2006, he has been a graduate student in School of Integrated Design Engineering, Graduate School of Science and Technology, Keio University. His research interests are mainly concentrated on software defined radio.